Learning a Static Bug Finder from Data

Yu Wang
State Key Laboratory of Novel Software Technology
Nanjing University
Nanjing, Jiangsu 210023, China
yuwang_cs@nju.edu.cn

Fengjuan Gao
State Key Laboratory of Novel Software Technology
Nanjing University
Nanjing, Jiangsu 210023, China
fjgao@smail.nju.edu.cn

Linzhang Wang
State Key Laboratory of Novel Software Technology
Nanjing University
Nanjing, Jiangsu 210023, China
lzwang@nju.edu.cn

Ke Wang*
Visa Research
Visa Inc.
Palo Alto, CA , USA
kewang@visa.com

Abstract

We present an alternative approach to creating static bug finders. Instead of relying on human expertise, we utilize deep neural networks to train static analyzers directly from data. In particular, we frame the problem of bug finding as a classification task and train a classifier to differentiate the buggy from non-buggy programs using Graph Neural Network (GNN). Crucially, we propose a novel interval-based propagation mechanism that leads to a significantly more efficient, accurate and scalable generalization of GNN.

We have realized our approach into a framework, NEURSA, and extensively evaluated it. In a cross-project prediction task, three neural bug detectors we instantiate from NEURSA are effective in catching null pointer dereference, array index out of bound and class cast bugs in unseen code. We compare NEURSA against several static analyzers (*e.g.* Facebook Infer and Pinpoint) on a set of null pointer dereference bugs. Results show that NEURSA is more precise in catching the real bugs and suppressing the spurious warnings. We also apply NEURSA to several popular Java projects on GitHub and discover 50 new bugs, among which 9 have been fixed, and 3 have been confirmed.

CCS Concepts •**Software and its engineering** → **Software notations and tools; General programming languages;**

1 Introduction

Static analysis is an effective technique to catch bugs early when they are cheap to fix. Unlike dynamic analysis, static analysis reasons about every path in a program, offering formal guarantees for its run-time behavior. As an evidence of their increasing maturity and popularity, many static analyzers have been adopted by major tech companies to prevent bugs leaked to their production code. Examples include Google's Tricorder [25], Facebook's Getafix [28] and Zoncolan, and Microsoft's Visual Studio IntelliCode.

Despite the significant progress, static analyzers suffer from several well-known issues. One, in particular, is the high false positive

---

*Ke Wang is the corresponding author.

rate which tends to overshadow true positives and hurt usability. The reason for this phenomenon is well-known: all nontrivial program properties are mathematically undecidable, meaning that automated reasoning of software generally must involve approximation. On the other hand, problems of false negatives also need to be dealt with. Recently, Habib and Pradel [13] investigated how effective the state-of-the-art static analyzers are in handling a set of real-world bugs. Habib *et al.* show more than 90% of the bugs are missed, exposing the severity of false negatives.

To tackle the aforementioned weaknesses, this paper explores an alternative approach to create static bug checkers—neural bug detection. Our observation is bug patterns exist even for those targeted by static analyzers. Therefore, machine learning techniques offer a viable solution. The challenge though is how to design a model that is effective in catching such bug patterns, which are non-trivial and can even be quite complex. Although Graph Neural Networks (GNN) have seen success across many program analysis tasks [1, 19, 30], they have been utilized only to catch specialized, relatively syntactic bugs in variable naming [1], hence limited impact. To elevate GNN's capability to a sufficient extent for detecting semantic bugs, we invent a novel, efficient propagation mechanism based on graph intervals. Our insight is specializing GNN to exploit the program-specific graph characteristics enhances their capacity of learning complex programming patterns. Specifically, our propagation mechanism forces GNN to attend to certain code constructs to extract deep, semantic program features. Moreover, our propagation mechanism operates on hierarchical graphs to alleviate the scalability issues GNN often encounters when learning from larger graphs.

We realize our approach into a framework, called NEURSA, that is general (*i.e.* language-agnostic), and extensible (*i.e.* not restricted to certain bug types). NEURSA performs inter-procedural analysis for bug finding. The framework first automatically scrapes training data across multiple project corpus, creating a large set of buggy and clean code examples; then trains a model to differentiate between these two; and finally uses the trained model for detecting bugs in previously unseen code. We present three neural bug detectors based on NEURSA targeting null pointer dereference, array index out of bound and class cast exceptions. Figure 1-3 depict three real bugs (from the dataset introduced by Ye et al. [38] and Just et al. [17]) that are caught by our neural bug detectors. In principle, extending NEURSA to create new bug detectors only requires the bug type information as the entire workflow will be automatically performed by NEURSA. In theory, compared to the soundy static

```
1  private MavenExecutionResult doExecute(
2      MavenExecutionRequest request) {
3      ...
4      projectDependencyGraph = createProjectDependencyGraph(
5          projects,request,result,true);
6
7      session.setProjects(projectDependencyGraph.getSortedProjects());
8
9      if (result.hasExceptions())
10         return result;
11     ...
12 }
```

Figure 1. A null pointer dereference bug (bugs-dot-jar_MNG-5613_bef7fac6). The presence of the exception handling routine at line 9-10 indicates the function at line 4 may throw an exception, in which case the value of `projectDependencyGraph` is likely to be null; subsequently, a null pointer dereference will be triggered at line 7.

```
1  public JavaElementLine(ITypeRoot element, int lineNumber,
2      int lineStartOffset) throws CoreException {
3      ...
4      IBuffer buffer = element.getBuffer();
5      ...
6      int length = buffer.getLength();
7      int i = lineStartOffset;
8
9      char ch = Array.getChar(buffer,i);
10     ...
11     while (i < length &&
12         !IndentManipulation.isLineDelimiterChar(ch)) {
13         ...
14         ch = Array.getChar(buffer, ++i);
15     ...
16 }
```

Figure 2. An array index out of bound bug (eclipse.jdt.ui-2f5e78c). Since the pre-incrementor at line 14 increments the value of `i` right before accessing the array `buffer`, an array index out of bound exception will be triggered in the iteration where `i` equals to `length-1`.

```
1  public static void addMissingReturnTypeProposals(
2      IInvocationContext context, IProblemLocation problem,
3      Collection<ICommandAccess> proposals) {
4      ...
5      if (parentType instanceof AbstractTypeDeclaration) {
6          boolean isInterface =
7              parentType instanceof TypeDeclaration &&
8              ((TypeDeclaration)parentType).isInterface();
9
10         if (!isInterface) {
11             String constructorName = ((TypeDeclaration)parentType).
12                 getName().getIdentifier();
13             ...
14 }
```

Figure 3. An class cast bug (eclipse.jdt.ui-c0e0634). If `isInterface` (line 6) is evaluated to false, it's possible `parentType` is not an instance of `TypeDeclaration`, in which case a class cast exception will be triggered at line 11.

analysis tools [21], our learner-based bug detectors are inherently unsound, however, their strength lies in their far lower cost of design (*i.e.* no human expertise is required), and comparable or even superior performance in practice.

Our approach significantly differs from almost all related work in the literature [1, 24, 34]. Specifically, we consider deep and semantic bugs that are proven to be hard even for state-of-the-art static analyzers instead of shallow and syntactic bugs targeted by

other works [1, 24, 34]. Additionally, NEURSA pinpoints a bug in a program to a line instead of predicting an entire file to be buggy or not [34].

We evaluate NEURSA by training its three instantiations on 30,000 methods extracted from hundreds of Java projects and detecting bugs in 1,700 methods from a different set of 13 Java projects. In total, our corpus amounts to 1,047,296 lines. We find that all neural bug detectors are effective with each achieving above 35% precision and 45% recall.

To further demonstrate the utility of NEURSA, we compare our neural bug detector with several static analysis tools (*e.g.* Facebook's Infer [5, 6], Pinpoint [29], *etc.*). Our comparison focuses on the performance of each checker in catching null pointer dereference bugs, the only kind of bugs that can be handled by all tools. Results show that our neural bug detector catches more bugs and produces less spurious warnings than any evaluated static analyzer. We have also applied our neural bug detectors to 17 popular projects on GitHub and discovered 50 new bugs, among which 9 have been fixed and 3 have been confirmed (fixes pending).

We make the following contributions:

- We propose a deep neural network based methodology for building static bug checkers. Specifically, we utilize GNN to train a classifier for differentiating buggy code from correct code.
- We propose a novel interval-based propagation model that significantly enhances the capacity of GNN in learning programming patterns.
- We design and implement a framework to streamline the creation of neural bug detectors The framework is open-sourced at https://github.com/anonymoustool/NeurSA.
- We publish our data set at https://figshare.com/articles/datasets_tar_gz/8796677 for the three neural bug detectors we built based on NEURSA to aid the future research activity.
- We present the evaluation results showing our neural bug detectors are highly precise in detecting the semantic bugs in real-world programs and outperform many flagship static analysis tools including Infer in catching null pointer dereference bugs.

2 Preliminary

First, we revisit the definition of connected, directed graphs. Then we give a brief overview of interval [2] and GNN [12], which our work builds on.

2.1 Graph

A graph $\mathcal{G} = (\mathcal{V}, \mathcal{E})$ consists of a set of nodes $\mathcal{V} = \{v_1, ..., v_m\}$, and a list of directed edge sets $\mathcal{E} = (\mathcal{E}_1, ..., \mathcal{E}_K)$ where K is the total number of edge types and $\mathcal{E}_k$ is a set of edges of type k. $E(v_s, v_d, k), k \in (1, ..., K)$ denotes an edge of type k directed from node v_s to node v_d. For graphs with only one edge type, E is represented as (v_s, v_d).

The immediate successors of a node v_i (denoted as $post(v_i)$) are all of the nodes v_j for which (v_i, v_j) is an edge in $\mathcal{E}$. The immediate predecessors of node v_j (denoted as $pre(v_j)$) are all of the nodes v_i for which (v_i, v_j) is an edge in $\mathcal{E}$.

A path is an ordered sequence of nodes $(v_j, ..., v_k)$ and their connecting edges, in which each $v_i \in pre(v_{i+1})$ for $i \in (j, ..., k-1)$. A closed path is a path in which the first and last nodes are the

---

Algorithm 1: Finding intervals for a given graph

Input: Graph $\mathcal{G}$, Node set $\mathcal{V}$
Output: Interval set $\mathcal{S}$

1 // v_0 is the unique entry node for the graph
2 H = $\{v_0\}$;
3 **while** $H \neq \emptyset$ **do**
4   // remove next h from H
5   h = H.pop();
6   I(h) = $\{h\}$;
7   // only nodes that are neither in the current interval nor any other interval will be considered
8   **while**
    $\{v \in \mathcal{V} \mid v \notin I(h) \land \nexists s(s \in \mathcal{S} \land v \in s) \land pre(v) \subseteq I(h)\} \neq \emptyset$
do
9   I(h) = I(h) $\cup$ { v };
10   // find next headers
11   **while** $\{v \in \mathcal{V} \mid \nexists s_1(s_1 \in \mathcal{S} \land v \in s_1) \land \exists m_1, m_2 \, (m_1 \in pre(v)$
    $\land \, m_2 \in pre(v) \land m_1 \in I(h) \land m_2 \notin I(h))\} \neq \emptyset$ **do**
12   H = H $\cup$ { v };
13     $\mathcal{S} = \mathcal{S} \cup I(h)$;

Figure 4. n-th order intervals and graphs. The set of intervals on $\mathcal{S}^1$ are $I^1(1)=\{1\}$, $I^1(2)=\{2\}$, $I^1(3)=\{3,4,5,6\}$, $I^1(7)=\{7\}$. $I^2(1)=\{1\}$ and $I^2(2)=\{2,7,8\}$ are the second order intervals. $I^3(1)=\{1,9\}$ and $I^4(10)=\{10\}$ are the only intervals on $\mathcal{S}^3$ and $\mathcal{S}^4$ respectively.

same. The successors of a node v_i (denoted as $post^*(v_i)$) are all of the nodes v_j for which there exists a path from v_i to v_j. The predecessors of a node v_j (denoted as $pre^*(v_j)$) are all of the nodes v_i for which there exists a path from v_i to v_j.

2.2 Interval

Introduced by Allen [2], an interval $I(h)$ is the maximal, single entry subgraph in which h is the only entry node and all closed paths contain h. The unique interval node h is called the interval head or simply the header node. An interval can be expressed in terms of the nodes in it: $I(h) = \{v_l, v_2, ..., v_m\}$.

By selecting the proper set of header nodes, a graph can be partitioned into a set of disjoint intervals. An algorithm for such a partition is shown in Algorithm 1. The key is to add to an interval a node only if all of whose immediate predecessors are already in the interval (Line 8 to 9). The intuition is such nodes when added to an interval keep the original header node as the single entry of an interval. To find a header node to form another interval, a node is picked that is not a member of any existing intervals although it must have a (not all) immediate predecessor being a member of the interval that is just computed (Line 11 to 12). We repeat the computation until reaching the fixed-point where all nodes are members of an interval.

The intervals on the original graph are called the first order intervals denoted by $I^1(h)$, and the graph from which they were derived is called first order graph (also called the set of first order intervals) $\mathcal{S}^1$ s.t. $I^1(h) \in \mathcal{S}^1$. By making each first order interval into a node and each interval exit edge into an edge, the second order graph can be derived, from which the second order intervals can also be defined. The procedure can be repeated to derive successively higher order graphs until the n-th order graph consists of a single node[1]. Figure 4 illustrates such a sequence of derived graphs.
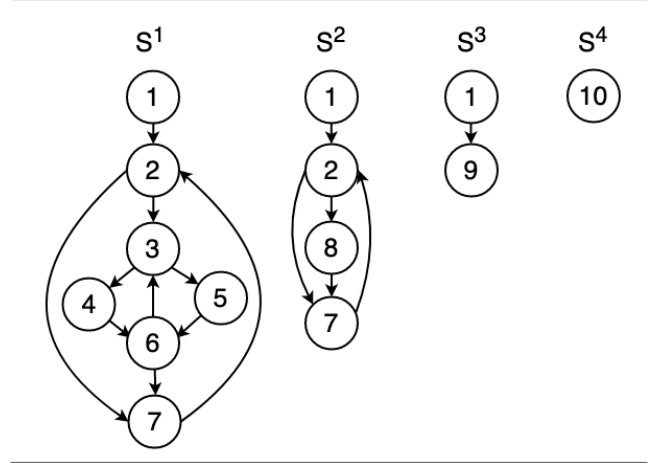
---

[1]Certain graphs can't be reduced to single nodes.

2.3 Graph Neural Network

Graph Neural Networks (GNN) [12, 27] is a specialized machine learning model designed to learn from graph data.

We extend the definition of a graph to include $\mathcal{M}$ (i.e. $G = (\mathcal{V}, \mathcal{E}, \mathcal{M})$). $\mathcal{M}$ is a set of vectors (or embeddings) $\{\mu_{v_1}, ..., \mu_{v_m}\}$, where each $\mu_v \in \mathbb{R}^d$ denotes the embedding of a node v in the graph. GNN updates node embeddings via a propagation model. The simplest yet most popular is synchronous message passing systems [3] introduced in distributed computing theory. Specifically, the inference is executed as a sequence of rounds: in each round, every node first sends messages to all of its neighbors, and then update its embedding by aggregating all incoming messages.

$$\mu_v^{(l+1)} = h(\{\mu_u^{(l)}\}_{u \in \mathcal{N}^k(v), k \in \{1,2,...,K\}}) \qquad (1)$$

$\mathcal{N}^k(v)$ denotes the neighbours that are connected to v with edge type k, i.e., $\mathcal{N}^k(v) = \{u|(u,v,k) \in \mathcal{E}\} \cup \{u|(v,u,k) \in \mathcal{E}\}$. $h(\cdot)$ denotes the aggregation function. We repeat the propagation for L steps to update μ_v to $\mu_v^{(L)}, \forall v \in \mathcal{V}$.

Some GNNs [30] compute a separate node embedding w.r.t. an edge type (i.e. $\mu_v^{(l+1),k}$ in Equation 2) before aggregating them into a final embedding (i.e. $\mu_v^{(l+1)}$ in Equation 3).

$$\mu_v^{(l+1),k} = \phi_1(\sum_{u \in \mathcal{N}^k(v)} \mathbf{W_1}\mu_u^{(l)}), \forall k \in \{1,2,...,K\} \qquad (2)$$

$$\mu_v^{(l+1)} = \phi_2(\mathbf{W_2}[\mu_v^{(l),1}, \mu_v^{(l),2}, ..., \mu_v^{(l),K}]) \qquad (3)$$

$\mathbf{W_1}$ and $\mathbf{W_2}$ are variables to be learned, and ϕ_1 and ϕ_2 are some nonlinear activation functions.

To further improve the model capacity, Li et al. [19] proposed Gated Graph Neural Network (GGNN). Their major contribution is a new instantiation of $h(\cdot)$ (Equation 1) with Gated Recurrent

Units [7]. The following equations describe how GGNN works:

$$\tilde{m}_v^l = \sum_{u \in \mathcal{N}(v)} f(\mu_u^{(l)}) \tag{4}$$

$$\mu_v^{(l+1)} = GRU(\tilde{m}_v^l, \mu_v^{(l)}) \tag{5}$$

To update the embedding of node v, Equation 4 computes a message $\tilde{m}_v^l$ using $f(\cdot)$ (*e.g.* a linear function) from the embeddings of its neighboring nodes $\mathcal{N}(v)$. Next a *GRU* takes $\tilde{m}_v^l$ and $\mu_v^{(l)}$—the current embedding of node v—to compute the new embedding, $\mu_v^{(l+1)}$ (Equation 5).

3 Interval-Based Propagation Mechanism

In this section, we present the Interval-Based Propagation Mechanism (IBPM), a new protocol that regulates how nodes exchange messages with their peers in a graph. In particular, we highlight the conceptual advantages IBPM enjoys over the existing propagation mechanism.

3.1 IBPM's Algorithm for Graph Propagation

We discuss two major issues existing works that apply GNN in program analysis suffer from.

Even though GNN has shown its generality by succeeding in a variety of problem domains (*e.g.* scene graph generation [37], traffic prediction [20], recommendation system [39], *etc.*), it can benefit from specializations designed to address the uniqueness of each problem setting, especially when dealing with programs, a fundamentally different data structure. However, prior works made little adjustment to accommodate such program-specific graph characteristics, resulted in a potential loss of model precision. Besides, scalability challenges can also hinder the generalization of GNN. That is when a graph has a large diameter; information has to be propagated over long distance, therefore, message exchange between nodes that are far apart becomes difficult.

IBPM is designed specifically to tackle the aforementioned weaknesses of GNN. To start with, programs are represented by their control flow graphs. More distinctively, propagation is only allowed on a subgraph defined by an interval. Since iteration statements (*i.e.* loops) often determines the formation of intervals (because loop back edge *e.g.* node 7 to node 2 in Figure 4 cuts off the loop header into a new interval), IBPM, in essence, attends to such loop structures when propagating on a control-flow graph. To enable the message-exchange between nodes that are far apart, IBPM switches onto a higher order graph, as such, involving more nodes to communicate within the same interval. On the other hand, by reducing the order of graph, IBPM restores the location propagation, and eventually recovers the node embeddings on the original control flow graph. Below we use the program in Figure 5, a function that computes the starting indices of the substring s1 in string s2, and its control-flow graph in Figure 4 to explain how IBPM works.

Depicted in Figure 5a, IBPM starts with the first order graph (*i.e.* the original control flow graph). As explained earlier, we restrict communication among nodes within the same interval. Consequently, node 3, 4, 5 and 6 will freely pass messages to the neighbors along their directed edges. On the contrary, node 1 and 2, which are alone in their respective intervals, will not contact any other node in the graph. Such propagation that occurs internal to an interval is carried out in the same manner as the standard propagation (Equation 1). Figure 5d highlights the part of the example

program that corresponds to the only active interval in the current step of IBPM. Apparently, IBPM focuses on learning from the inner loop while leaving the rest of the program unattended.

We then move onto the second order graph as shown in Figure 5b. Recall how a second order graph is derived. We compute a new node (*i.e.* node 8) to replace the only active interval on the first order graph (*i.e.* node 3, 4, 5 and 6). Equation 6 defines how to initialize node 8 or any other node that is created when IBPM transitions from lower-order to higher-order graphs.

$$\mu_w^{(0)} = \sum_{v \in I^i(h)} \alpha_v \mu_v^{(l)} \tag{6}$$

where w denotes the node created out of the interval $I^i(h)$ and α_v is defined by

$$\alpha_v = \frac{exp(\mu_v^{(l)})}{\sum\limits_{v \in I^i(h)} exp(\mu_v^{(l)})} \tag{7}$$

Due to the same restriction IBPM imposes, propagation on the second order graph now covers node 2, 7 and 8. Because node 8 can be deemed as a proxy of node 3-6, this propagation, in essence, covers all but node 1 on the first order graph. In other words, even though propagation is always performed within each interval, increasing the order of a graph implicitly expands the region of an interval, therefore facilitating more nodes to communicate. For visualization, Figure 5e highlights the part of the program—the nested loop structure—IBPM attends to at the current step.

Figure 5c shows the third step of IBPM, where propagation spans across the entire graph. Upon completion of the message-exchange between node 1 and 9, IBPM transitions back to the lower order graphs; interval nodes will be split back into the multitude of nodes from which they formed (*e.g.* node 9 to node 2, 7 and 8; node 8 to node 3-6). Equation below defines how to compute the initial embeddings for a node that is split from an interval. μ_w and α_v denote the same meaning in Equation 6.

$$\mu_v^{(0)} = \alpha_v \mu_w^{(l)}$$

Eventually, the node embeddings on the original control flow graph will be recovered. Worth mentioning recurring local propagation on the lower order graphs improves the accuracy of node embeddings by incorporating the previously accumulated global graph knowledge on the higher order graphs. In return, more precise modeling of the subgraphs also benefits the further global propagation across the entire graph. As the transitioning between local and global mode repeats, node embeddings will continue to be refined to reflect the properties of a graph.

3.2 Comparing IBPM to Standard Propagation

Structured Propagation As described in Section 3.1, IBPM works with a graph hierarchy, where each level attends to distinct, important code constructs in a program, such as the loops illustrated in Figure 5d and 5e. This is in stark contrast with the standard propagation mechanism, where program structure is largely ignored and messages spread across the entire graph. Intuitively, we believe by utilizing the program constructs to regulate the message exchange, IBPM improves the precision of GNN in learning program properties.
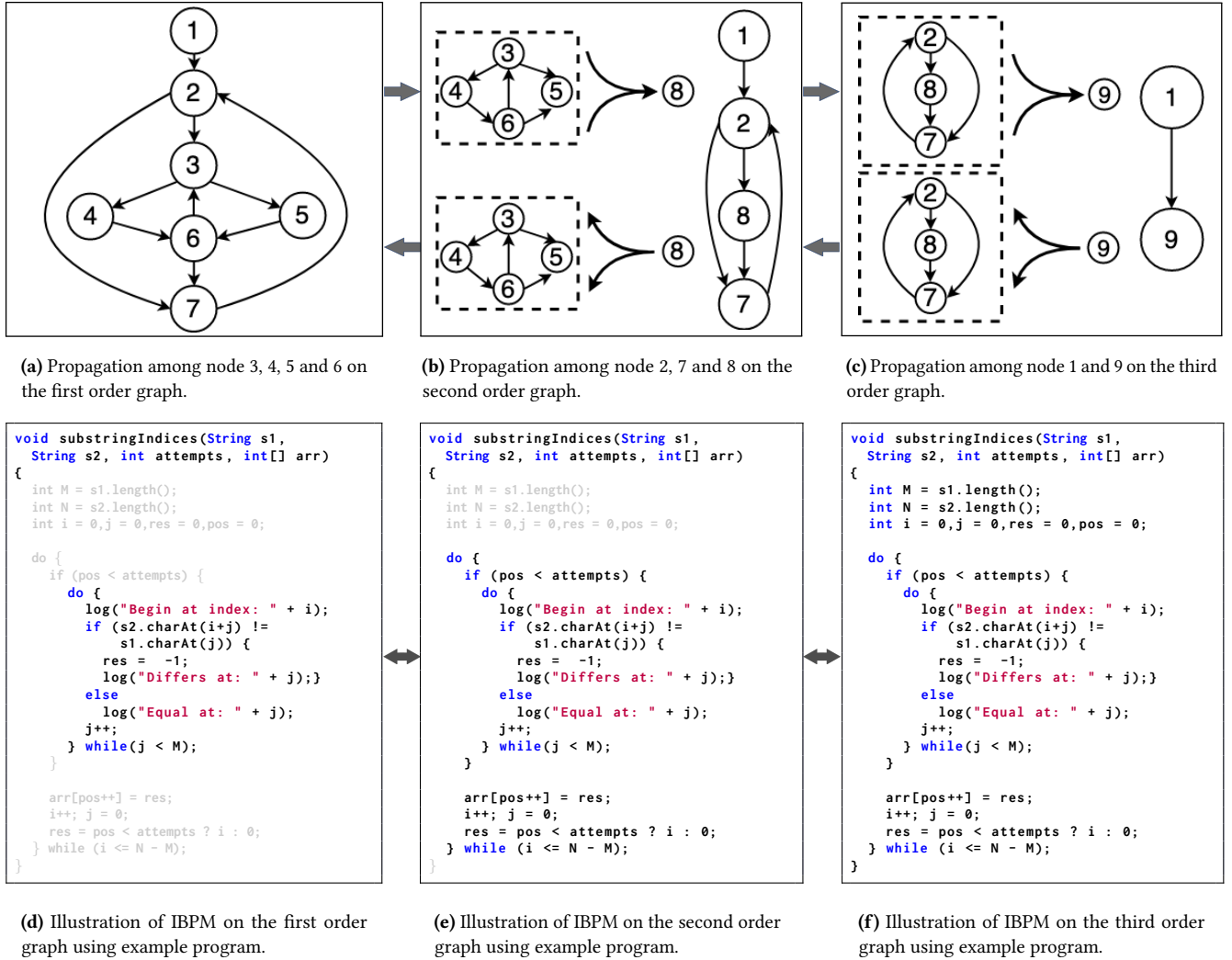
(a) Propagation among node 3, 4, 5 and 6 on the first order graph.

(b) Propagation among node 2, 7 and 8 on the second order graph.

(c) Propagation among node 1 and 9 on the third order graph.

```
void substringIndices(String s1,
  String s2, int attempts, int[] arr)
{
  int M = s1.length();
  int N = s2.length();
  int i = 0,j = 0,res = 0,pos = 0;

  do {
    if (pos < attempts) {
      do {
        log("Begin at index: " + i);
        if (s2.charAt(i+j) !=
          s1.charAt(j)) {
          res =  -1;
          log("Differs at: " + j);}
        else
          log("Equal at: " + j);
        j++;
      } while(j < M);
    }

    arr[pos++] = res;
    i++; j = 0;
    res = pos < attempts ? i : 0;
  } while (i <= N - M);
}
```

```
void substringIndices(String s1,
  String s2, int attempts, int[] arr)
{
  int M = s1.length();
  int N = s2.length();
  int i = 0,j = 0,res = 0,pos = 0;

  do {
    if (pos < attempts) {
      do {
        log("Begin at index: " + i);
        if (s2.charAt(i+j) !=
          s1.charAt(j)) {
          res =  -1;
          log("Differs at: " + j);}
        else
          log("Equal at: " + j);
        j++;
      } while(j < M);
    }

    arr[pos++] = res;
    i++; j = 0;
    res = pos < attempts ? i : 0;
  } while (i <= N - M);
}
```

```
void substringIndices(String s1,
  String s2, int attempts, int[] arr)
{
  int M = s1.length();
  int N = s2.length();
  int i = 0,j = 0,res = 0,pos = 0;

  do {
    if (pos < attempts) {
      do {
        log("Begin at index: " + i);
        if (s2.charAt(i+j) !=
          s1.charAt(j)) {
          res =  -1;
          log("Differs at: " + j);}
        else
          log("Equal at: " + j);
        j++;
      } while(j < M);
    }

    arr[pos++] = res;
    i++; j = 0;
    res = pos < attempts ? i : 0;
  } while (i <= N - M);
}
```

(d) Illustration of IBPM on the first order graph using example program.

(e) Illustration of IBPM on the second order graph using example program.

(f) Illustration of IBPM on the third order graph using example program.

Figure 5. Interval-Based Propagation Mechanism.

Scalable Propagation   We prove in theory IBPM also enjoys scalability advantage over the standard propagation mechanism. By scalability, we mean the number of messages that have been passed in total until the graph is sufficiently propagated. Since determining the threshold of sufficient propagation is beyond the scope of this paper, we make reasonable approximations to assist our proof. For simplicity, we assume directed, connected graphs which consist of distinct nodes and homogeneous edges, and synchronous message passing scheme in all definitions, theorems, and proofs.

Definition 3.1. (Distance) Given two nodes v_i and v_j on a graph $\mathcal{G}$, their distance, denoted by $\theta(v_i, v_j)$, is the length of the shortest path from v_i to v_j on $\mathcal{G}$.

Definition 3.2. (Diameter) The diameter of a graph $\mathcal{G}$, $\pi(\mathcal{G})$, is the longest distance between any two nodes on $\mathcal{G}$. Assuming $\mathcal{V}$ is the set of nodes on $\mathcal{G}$.

$$\pi(\mathcal{G}) = \max_{v_i, v_j \in \mathcal{V}} \theta(v_i, v_j)$$

We define the point of sufficient propagation as follows.

Definition 3.3. (Fixed Point) Given a graph $\mathcal{G} = (\mathcal{V}, \mathcal{E})$, associate each node $v \in \mathcal{V}$ with a set σ_v, which is initialized to contain the node itself, denoted by $\sigma_v^0 = \{v\}$. After the l-th round of message passing, σ_v^l is updated to $\bigcup_{u \in \mathcal{N}(v)} \sigma_u^{l-1}$, where $\mathcal{N}(v)$ refers to the neighbouring nodes of v. The propagation is said to reach the fixed point on $\mathcal{G}$ after l-th round of message passing iff (1) $\forall l' \geq l$, $\forall v \in \mathcal{V}$, $\sigma_v^l = \sigma_v^{l'}$; and (2) $\nexists l' < l$, $\forall l'' \geq l'$, $\forall v \in \mathcal{V}$, $\sigma_v^{l'} = \sigma_v^{l''}$.

Theorem 3.4 (Distance Measure). *Given two nodes v_i and v_j on a graph (hereinafter assuming all edges are of unit length), if σ_{v_j} contains v_i only after the l-th round of message passing, that is $\forall l' < l$, $v_i \notin \sigma_{v_j}^{l'}$ and $\forall l' \geq l$, $v_i \in \sigma_{v_j}^{l'}$, then $\theta(v_i, v_j) = l$.*

Proof. Assume otherwise s.t. $\theta(v_i, v_j) = l' \wedge l \neq l'$. Synchronous message passing system in essence enumerates all possible paths between any two nodes on the graph. In particular, all paths of length l will be enumerated in l-th round of message passing. If $\theta(v_i, v_j) = l'$, then l' rounds would have been needed, after which

σ_{v_j} contains v_i, which contradicts the assumption σ_{v_j} contains v_i after the l-th round of message passing. □

Theorem 3.5 (Scalability Measure). *Given a graph $\mathcal{G} = (\mathcal{V}, \mathcal{E})$, the number of messages that have been sent by all nodes in $\mathcal{V}$ until the propagation reaches fixed point on $\mathcal{G}$ equals to $\pi(\mathcal{G}) * |\mathcal{E}|$.*

Proof. Because synchronous message passing system has $|\mathcal{E}|$ message sent in each round on directed graphs. So it suffices to prove that $\pi(\mathcal{G})$ rounds of message passing are needed until propagation reaches the fixed point. Assume otherwise, reaching the fixed point on $\mathcal{G}$ takes l' rounds:

(a) $l' > \pi(\mathcal{G})$. This indicates $\exists v_i \in \mathcal{V}, \exists v_j \in \mathcal{V}, \forall l'' < l', v_i \notin \sigma_{v_j}^{l''} \wedge v_i \in \sigma_{v_j}^{l'}$. According to Theorem 3.4, then $\theta(v_i, v_j) = l'$. Since $l' > \pi(\mathcal{G})$, therefore contradicting the Definition 3.2.

(b) $l' < \pi(\mathcal{G})$. This indicates $\nexists v_i \in \mathcal{V}, \nexists v_j \in \mathcal{V}, \nexists l'' > l', \forall l''' < l'', v_i \notin \sigma_{v_j}^{l'''} \wedge v_i \in \sigma_{v_j}^{l''}$. According to Theorem 3.4, then $\nexists v_i \in \mathcal{V}, \nexists v_j \in \mathcal{V}, \nexists l'' > l', \theta(v_i, v_j) = l''$, and therefore $l' \geq \pi(\mathcal{G})$, which contradicts the assumption $l' < \pi(\mathcal{G})$. □

Similarly, we define the saturation point of IBPM.

Definition 3.6. (Fixed Point for IBPM) Given the first order graph $\mathcal{S}^1$, and successively derived higher order graphs, $\mathcal{S}^2, \mathcal{S}^3, ..., \mathcal{S}^n$ ($\mathcal{S}^n$ represents the highest order graph), propagation transitions from $\mathcal{S}^i$ to $\mathcal{S}^{i+1}$ (or $\mathcal{S}^{i-1}$) only after the fixed point on all intervals in $\mathcal{S}^i$ has been reached (according to the Definition 3.3). In addition, $\sigma_{v^{i+1}}^0$ of a new node v^{i+1} on $\mathcal{S}^{i+1}$ is initialized to $\bigcup_{u \in I^i(v)} \sigma_u^l$, where $I^i(v)$ denotes the interval from which v^{i+1} is created, and $l = \pi(I^i(v))$. As for a new node v^{i-1} on $\mathcal{S}^{i-1}$, $\sigma_{v^{i-1}}^0$ is initialized to $\{v^{i-1}\}$. The whole process is said to reach fixed point iff the propagation successively transitions from $\mathcal{S}^1$ to $\mathcal{S}^n$ and back to $\mathcal{S}^1$, on which subsequent propagation also reaches fixed point.

Theorem 3.7 (Scalability Measure for IBPM). *Given $\mathcal{S}^1, \mathcal{S}^2, ..., \mathcal{S}^n$ and their respective member intervals $I^1(h_1^1), ..., I^1(h_{|\mathcal{S}^1|}^1); I^2(h_1^2), ..., I^2(h_{|\mathcal{S}^2|}^2); I^n(h_1^n), ..., I^n(h_{|\mathcal{S}^n|}^n)$, the number of messages that have been sent until IBPM reaches fixed point equals to*

$$\left(\sum_{j=1}^{n-2} \sum_{i=1}^{|\mathcal{S}^j|} 2 * \pi(I^j(h_i^j)) * |\mathcal{E}_{I^j(h_i^j)}| \right) + \pi(\mathcal{S}^{n-1}) * |\mathcal{E}_{\mathcal{S}^{n-1}}| \quad (8)$$

if $\mathcal{S}^n$ is a single node, otherwise

$$\left(\sum_{j=1}^{n-1} \sum_{i=1}^{|\mathcal{S}^j|} 2 * \pi(I^j(h_i^j)) * |\mathcal{E}_{I^j(h_i^j)}| \right) + \pi(\mathcal{S}^n) * |\mathcal{E}_{\mathcal{S}^n}|$$

$\mathcal{E}_g$ denotes the set of edges in g in both formulas.

Proof. Break IBPM into sub-propagation on each interval at each order of graph. Therefore, the number of messages sent in total can be computed by summing up the messages sent during each sub-propagation. Since all assumptions still hold, Theorem 3.5 can be applied to derive the proof. □

Below we compare the scalability of two propagation mechanism. First, we consider the case where $\mathcal{S}^n$ is a single node. Add another

$\pi(\mathcal{S}^{n-1}) * |\mathcal{E}_{\mathcal{S}^{n-1}}|$ to Equation 8 leads to:

$$\left(\sum_{j=1}^{n-2} \sum_{i=1}^{|\mathcal{S}^j|} 2 * \pi(I^j(h_i^j)) * |\mathcal{E}_{I^j(h_i^j)}| \right) + \pi(\mathcal{S}^{n-1}) * |\mathcal{E}_{\mathcal{S}^{n-1}}| <$$
$$\left(\sum_{j=1}^{n-2} \sum_{i=1}^{|\mathcal{S}^j|} 2 * \pi(I^j(h_i^j)) * |\mathcal{E}_{I^j(h_i^j)}| \right) + 2 * \pi(\mathcal{S}^{n-1}) * |\mathcal{E}_{\mathcal{S}^{n-1}}| \quad (9)$$

Absorb $2 * \pi(\mathcal{S}^{n-1}) * |\mathcal{E}_{\mathcal{S}^{n-1}}|$ into the sum at the right hand side of Equation 9 gives

$$\left(\sum_{j=1}^{n-2} \sum_{i=1}^{|\mathcal{S}^j|} 2 * \pi(I^j(h_i^j)) * |\mathcal{E}_{I^j(h_i^j)}| \right) + \pi(\mathcal{S}^{n-1}) * |\mathcal{E}_{\mathcal{S}^{n-1}}| <$$
$$\sum_{j=1}^{n-1} \sum_{i=1}^{|\mathcal{S}^j|} 2 * \pi(I^j(h_i^j)) * |\mathcal{E}_{I^j(h_i^j)}| \quad (10)$$

To simply, assume

$$\forall j \in [1, n-1], \forall i \in [1, |\mathcal{S}^j|], \pi(I^j(h_i^j)) = \tau$$

then

$$\sum_{j=1}^{n-1} \sum_{i=1}^{|\mathcal{S}^j|} 2 * \pi(I^j(h_i^j)) * |\mathcal{E}_{I^j(h_i^j)}| = 2 * \tau * \sum_{j=1}^{n-1} \sum_{i=1}^{|\mathcal{S}^j|} |\mathcal{E}_{I^j(h_i^j)}| \quad (11)$$

Because $\sum_{j=1}^{n-1} \sum_{i=1}^{|\mathcal{S}^j|} |\mathcal{E}_{I^j(h_i^j)}| \leq |\mathcal{E}|$. In particular, the equivalence establishes when none of the intervals at any order of graph that has multiple exit edges to the same external node. So we derive

$$2 * \tau * \sum_{j=1}^{n-1} \sum_{i=1}^{|\mathcal{S}^j|} |\mathcal{E}_{I^j(h_i^j)}| \leq 2 * \tau * |\mathcal{E}| \quad (12)$$

Linking Equation 9-12, we derive

$$\left(\sum_{j=1}^{n-2} \sum_{i=1}^{|\mathcal{S}^j|} 2 * \pi(I^j(h_i^j)) * |\mathcal{E}_{I^j(h_i^j)}| \right) + \pi(\mathcal{S}^{n-1}) * |\mathcal{E}_{\mathcal{S}^{n-1}}| <$$
$$2\tau * |\mathcal{E}|$$

Essentially, we have estimated an upper bound of the scalability measure for IBPM: $2\tau * |\mathcal{E}|$. The same upper bound can also be derived for the other case where $\mathcal{S}^n$ is not a single node. Comparing with Theorem 3.5's result: $\pi(\mathcal{G}) * |\mathcal{E}|$, IBPM is more scalable than the standard propagation mechanism since the diameter of an interval is generally small (*i.e.* around 2 on control flow graphs according to our large-scale evaluation). When the size of a graph increases, the size of an interval mostly stays as a constant, therefore IBPM outperforms the standard propagation by an even wider margin. Overall, using sensible approximations, we have proved IBPM is superior to the standard propagation in the scalability regard.

4 Framework

This section presents NeurSA, a framework for creating various kinds of neural bug detectors.

4.1 Overview of NeurSA

Figure 6 depicts the overview of NeurSA. We split NeurSA's workflow into four parts and describe each one below.
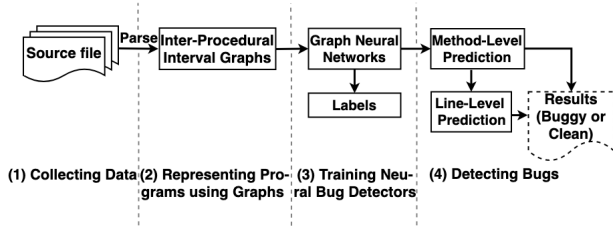
Figure 6. NEURSA's Workflow.

(1) **Collecting Data:** We extract programs from the codebases of real-world projects. We obtain bug labels by cross-referencing bug reports and the commit history of the same project.

(2) **Representing Programs Using Graphs:** We construct the control flow graph for each method. To facilitate NEURSA to pinpoint a bug in a method, we break each node denoting a basic block into multiple nodes each of which represents a non-control statement. We also stitch the control flow graphs of caller and callee to aid inter-procedural analysis.

(3) **Training Neural Bug Detectors:** We train neural bug detectors using graph neural networks. In particular, we propose a novel interval-based propagation mechanism that significantly enhances the capacity of GNN in learning programming patterns.

(4) **Bug Detection:** Finally, we detect bugs in unseen code using the model we have trained.

4.2 Data Generation

We use bug databases proposed by the prior works [17, 26, 32, 38] to generate our dataset. All databases provide a rich set of meta-information on each bug they contain (*e.g.* detailed bug descriptions, links to actual commits of bug fixes, projects bug reports, *etc.*). We rely on such information to extract buggy methods and identify bug types. For example, given a bug description "*Fixing Bugzilla#2206...*", we search in the bug reports using the id *#2206* to retrieve the details of the bug, against which we match pre-defined keywords to determine the type of the bug. Next, we refer to the code commit to find out bug locations, specifically, we consider the lines that are modified by this commit to be buggy and the rest to be clean. We acknowledge the location of a bug and its fix may not be precisely the same thing. However, given the quality and maturity of the codebases we work with, our assumptions are reasonable. After extracting a buggy method, we choose from the same project several syntactically closest correct methods *w.r.t.* the tree edit distance between their abstract syntax trees.

4.3 Representing Programs with Graphs

We represent each method using its control flow graph. Besides, we split a graph node representing a basic block into a number of nodes, each of which represents a single statement. This variation enables the localization of bugs at the level of lines. To further enhance the expressiveness of our graph representation, we take the following measures: (1) we incorporate a new type of edges to represent the data dependency among variables. Specifically, we connect nodes with data dependency edges if the statements they represent exhibit a dependency relationship. Note that data dependency edges do not contribute to partitioning graphs into intervals. They only facilitate the local propagation within each interval. (2) we also add variable

types into the mix. Given a variable var, we consider not only its actual type $\tau(var)$ but also all the supertypes of $\tau(var)$, denoted by $\tau^*(var) = \bigcup_{i=1}^{i=n} \tau^i(var)$, where $\tau^i(var) = \{\tau | \bigcup_{\omega \in \tau^{i-1}(var)} \omega$ implements $\tau\}$ with a base case $\tau^1(v) = \{\tau | \tau(var)$ implements type $\tau\}$. $\tau^n(var)$ signals the most general type (*e.g.* Object in Java).

Due to the static nature of each non-control statement, we resort to recurrent neural networks—suitable for modeling sequentially data—to learn the initialization for each node in the graph. In particular, we treat a statement as a sequence of tokens. After each token is embedded into a numerical vector (similar to word embeddings [22]), we feed the entire token sequence into the network and extract its final hidden state as the initial node embedding.

We stitch the graphs of all callers (*i.e.* methods invoking the target method) and callees (*i.e.* methods invoked by the target method) to that of each target method to support inter-procedural analysis. In particular, we connect the node of method invocation inside of the caller to that of the entry point inside of the callee. Node labels obtained for each graph will be kept on the merged graph for neural bug detectors to predict. Worth mentioning our graph representation is independent of the type of the bug detector we train. In other words, a graph only presents the semantic representation of a program, it's the responsibility of a bug detector to learn the patterns *w.r.t.* the type of bugs it's interested in.

4.4 Training and Testing Neural Bug Detectors

Given the method representations we derived, we train a classifier using GNN with IBPM. In particular, different types of bug detectors will be trained and applied separately to catch bugs in the unseen code. Internally, each neural bug detector is trained in two steps. First, we train a feed-forward neural network [31] on top of method embeddings computed from GNN (*i.e.* aggregation of the node embeddings) to predict if a method is buggy or not. If it is, we will use the same network to predict the buggy lines. Our rationale is graph as a whole provides stronger signals for models to determine the correctness of a method. Correct methods will be refrained from further predictions, resulted in fewer false warnings to be emitted. On the other hand, if a method is indeed predicted to be buggy, our model will then pick the top N statements according to their probabilities of being buggy. The benefit of this prediction mode is to provide flexibility for developers to tune their analysis toward either producing less false warnings or identifying more bugs.

5 Evaluation

This section presents an extensive evaluation of the three neural bug detectors we instantiate from NEURSA. First, we evaluate the performance of each neural bug detector. Next, we highlight the improved model capacity IBPM attributes to. Finally, we show how our neural bug detector fares against several static analysis tools in catching null pointer dereference bugs, followed by a summary of applying NEURSA to catch bugs in the wild.

5.1 Implementation

Due to the popularity and availability of Java datasets, we target semantic bugs in Java programs. For a different language, NEURSA only requires a front-end analyzer that extracts the control flow graphs for programs in the new language, the rest of the workflow is language-agnostic. We construct the control flow and interval

graphs using Spoon [23], an open-source library for analyzing Java source code. To efficiently choose correct methods to pair with each buggy method, we run DECKARD [16], a clone detection tool adopting an approximation of the shortest tree edit distance algorithm to identify similar code snippets.

We realize our IBPM-based GNN based on GGNN's implementation [19]. All neural bug detectors are implemented in Tensorflow. All RNNs built in the model have 1 recurrent layer with 100 hidden units. Each token in the vocabulary is embedded into a 100-dimensional vector. We experimented with other model configurations (*e.g.* more recurrent layers, hidden units, *etc.*) and did not obtain better results. We use random initialization for weight initialization. We train the neural bug detectors using the Adam optimizer [18]. All experiments are performed on a 3.7GHz i7-8700K machine with 32GB RAM and NVIDIA GTX 1080 GPU.

5.2 Experiment Setup

We assemble a dataset according to the procedure described in Section 4.2. Table 1 shows the details: the projects from which we extract the code snippet, a brief description of their functionality, size of their codebase, and the number of buggy methods we extract from each project. We maintain approximately 3:1 ratio between the correct and buggy methods across each bug type within each project. To enrich the set of AIE (Array Index Out of Bound Exception) and CCE (Class Cast Exception) bugs, we create synthetic buggy examples based on a collection of highly-rated and actively maintained projects from BugSwarm [32]. In particular, we first randomly pick methods that contain either array access or class cast operations, and then strip away the bounds or type checks. The number in parenthesis depicts how many buggy examples we synthesized for AIE and CCE. Note that all synthetic bugs are used for the training purpose only, and all bugs in the test set are real. We also make certain clean methods that are paired with synthetic buggy examples are chosen from other methods rather than their original version (*i.e.* with the bounds or type checks). We evaluate NEURSA on a standard classification task, that is, predicting each line in a method in the test set to be buggy or not. Since we deal with a largely unbalanced dataset, we forgo the accuracy metric and opt for Precision, Recall, and F1 Score, metrics are commonly used in defect prediction literature [24, 34].

As a baseline, we select standard GGNN [1, 19], a predominate deep learning model in the domain of programming. In particular, we re-implemented the program encoding scheme proposed by Allamanis et al. [1], a graph representation built of top of the AST with additional edges denoting variable types, data, control flow dependencies, *etc.*

5.3 Performance Measurement

We build two sets of neural bug detectors based on NEURSA and the baseline. Each set includes three models, each of which deals with null pointer dereference, array index out of bound and class casting bugs respectively.

Evaluating models using proposal metrics   Table 2–10 depicts the precision, recall, and F1 for all neural bug detectors. We set out to examine the impact of the depth of inlining on the performance of each bug detector. In particular, each row in a table shows the result of a neural bug detector that is trained either using the baseline model or NEURSA. The number in parenthesis is the depth

of inlining. Specifically, 0 means no inlining, 1 inlines all methods that are invoking or invoked by the target methods, and 2 further inlines all callers and callees of each method that is inlined by 1. Exceeding the depth of 2 has costly consequences. First, most data points will have to be filtered out for overflowing the GPU memory. Moreover, a significant portion of the remaining ones would also have to be placed in a batch on its own, resulted in a dramatic increase in training time. Methods in the test set are inlined as deep as those in the training set to maintain a consistent distribution across the entire dataset. We also make certain each buggy method is only inlined once to prevent a potential date duplicate issue. Columns in each table correspond to three prediction modes in which NEURSA picks 1, 3 or 5 statements to be buggy after a method is predicted to be buggy.

Overall, NEURSA consistently outperforms the baseline across all bug types using all proposed metrics. In particular, NEURSA beats the baseline by around 10% across all bugs types in F1 score. Regarding the impact of the depth of inlining, we find that increasing the depth mostly but not always leads to improved performance of either NEURSA or the baseline. The reason is, on one hand, models will benefit from a more complete program representation thanks to the inlining. On the other hand, exceedingly large graphs hinders the generalization of GNNs, resulted in degraded performance of the neural bug detectors.

Investigating models scalability   We divide the entire test set into ten subsets, each of which consists of graphs of similar size. We then investigate how models perform on each subset starting from the smallest to the largest graphs. We fix the depth of inlining to be 2, which provides the largest variation among all graphs in terms of the size. Figure 7a depicts the F1 score for NEURSA and the baseline under top-3 prediction mode (top-1 and top-5 yield similar results). Initially, NEURSA achieves slightly better results on the subset of small graphs; later as the size of graphs increases, NEURSA is significantly more resilient with its prediction than the baseline. Overall, we conclude bug detectors built out of NEURSA are more scalable.

Measuring training efficiency   Since all models make instantaneous predictions (*e.g.* around 800 examples per second), we only measure the training speed of NEURSA and the baseline. Again, we fix the depth of inlining to be 2, which presents the biggest challenges in training efficiency. Figure 7b shows the *test* F1 score (average across top-1, 3 and 5 prediction modes) over training time for NEURSA and the baseline on null pointer dereference bugs (Other two bug types are much easier to train). NEURSA's bug detector achieves results that are as 50% as good as its final results under half an hour, and results that are as 95% as good under 1 hour, while both being substantially higher than the best results of the baseline models. Our model achieves its best results around the 1 hour mark.

5.4 Contribution of IBPM

We aim to precisely quantify IBPM's contribution to the learning capacity of the GNN. In particular, we re-implement NEURSA by replacing its IBPM with the standard propagation mechanism. In other words, we perform a head-to-head comparison between the two propagation mechanisms while the rest of the model architecture is held the same. Figure 7c shows how the test F1 scores of both configurations vary with the number of first order intervals

Table 1. Details about our dataset. NPE, AIE, and CCE stand for null pointer dereference, array index out of bound and class cast exceptions respectively. Numbers in parenthesis records the number of synthetic bugs we created for AIE and CCE.

Dataset	Projects	Description	Size (KLoC)	Number of Buggy Methods		
				NPE	AIE	CCE
Test	Lang	Java lang library	50	7	5	2
	Closure	A JavaScript checker and optimizer.	260	18	0	0
	Chart	Java chart library	149	17	7	0
	Mockito	Mocking framework for unit tests	45	14	5	23
	Math	Mathematics and statistics components	165	16	17	3
	Accumulo	Key/value store	194	6	0	0
	Camel	Enterprise integration framework	560	17	1	1
	Flink	System for data analytics in clusters	258	13	0	0
	Jackrabbit-oak	hierarchical content repository	337	23	1	1
	Log4j2	Logging library for Java	70	29	1	2
	Maven	Project management and comprehension tool	62	6	0	0
	Wicket	Web application framework	206	7	1	8
	Birt	Data visualizations platform	1,093	678	129	154
	Number of Buggy Methods in Total for Test			793	167	192
	Number of Methods in Total for Test			3,000	600	800
Training	JDT UI	User interface for the Java IDE	508	897	63	156
	SWT	Eclipse Platform project repository	460	276	136	26
	Platform UI	User interface and help components of Eclipse	595	920	72	194
	AspectJ	An aspect-oriented programming extension	289	151	14	19
	Tomcat	Web server and servlet container	222	111	18	28
	from BugSwarm	61 projects on GitHub	5,191	156	20	3
	from BugSwarm	250 projects on GitHub	19,874	(0)	(2,356)	(1,998)
	Number of Buggy Methods in Total for Training			2,511	2,679	2,424
	Number of Methods in Total for Training			10,000	10,000	10,000
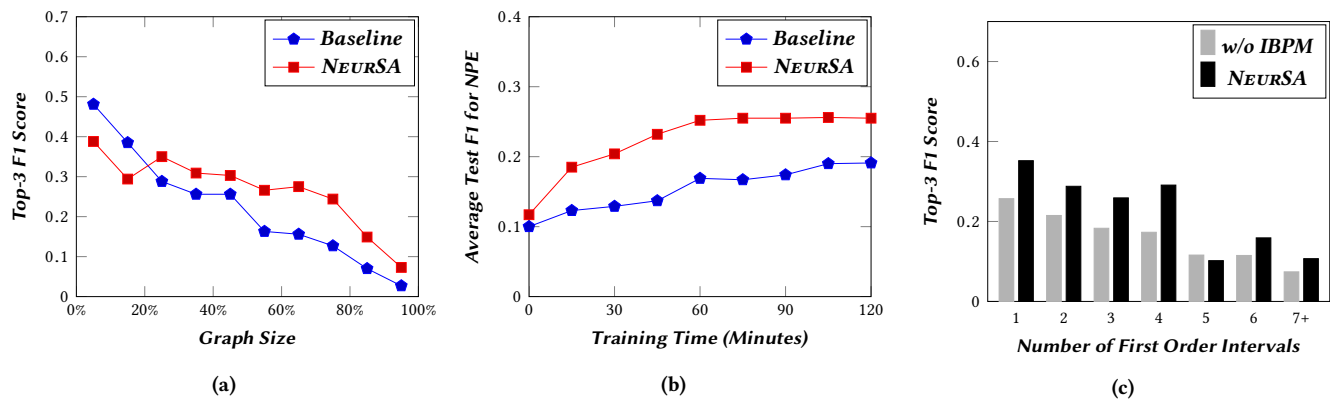
Figure 7. Experiment results.

in top-3 prediction mode (top-1 and top-5 yield similar results). For the same reason, the depth of inlining is fixed to be 2. Given the same number of the first order intervals, IBPM performs better than the standard propagation mechanism across the board. Apart from the apparent scalability advantage IBPM displays over the standard propagation mechanism, IBPM achieves better results even when the number of intervals is small, thanks to its exploitation of the program-specific graph characteristics.

5.5 Futher Evaluation of NEURSA

In general, static analyzers can be classified into two categories: soundy and unsound. The former refers to tools that are sound by design but make unsound choices for utility concerns, whereas

the latter is often built out of pattern matching techniques that do not concern themselves with soundness. Intending to cover both flavors, we pick soundy tools: Facebook Infer [5, 6], Pinpoint [29] and BugPicker, and another unsound tool: SpotBugs (the successor of FindBugs [15]).

We emphasize that our work makes no claims of advancing the theory of sound static analysis, therefore this experiment solely focuses on studying the utility of each tool in practice. We examine the performance of each checker in catching null pointer dereference bugs, which happen to be the only type of bugs all tools support.

To keep the engineering load manageable, we randomly pick 75 bugs out of seven projects from defect4j and bugs.jar, two most

Table 2. Precision in predicting NPE.

Methods	Top-1	Top-3	Top-5
Baseline (0)	0.209	0.147	0.117
Baseline (1)	*0.285*	0.166	0.131
Baseline (2)	0.218	0.138	0.101
NEURSA (0)	0.326	0.174	0.138
NEURSA (1)	**0.351**	0.167	0.130
NEURSA (2)	0.305	0.164	0.136
Gain	**0.351** - *0.285* = 0.066		

Table 3. Recall in predicting NPE.

Methods	Top-1	Top-3	Top-5
Baseline (0)	0.243	0.373	*0.450*
Baseline (1)	0.171	0.252	0.302
Baseline (2)	0.210	0.337	0.375
NEURSA (0)	0.282	0.374	0.447
NEURSA (1)	0.329	0.431	**0.507**
NEURSA (2)	0.304	0.402	0.500
Gain	**0.507** - *0.450* = 0.057		

Table 4. F1 score in predicting NPE.

Methods	Top-1	Top-3	Top-5
Baseline (0)	*0.224*	0.211	0.186
Baseline (1)	0.214	0.201	0.183
Baseline (2)	0.214	0.196	0.159
NEURSA (0)	0.303	0.238	0.211
NEURSA (1)	**0.339**	0.241	0.207
NEURSA (2)	0.304	0.233	0.214
Gain	**0.339** - *0.224* = 0.115		

Table 5. Precision in predicting AIE.

Methods	Top-1	Top-3	Top-5
Baseline (0)	*0.286*	0.124	0.106
Baseline (1)	0.218	0.112	0.095
Baseline (2)	0.215	0.134	0.088
NEURSA (0)	0.269	0.159	0.113
NEURSA (1)	0.308	0.134	0.097
NEURSA (2)	**0.362**	0.131	0.110
Gain	**0.362** - *0.286* = 0.076		

Table 6. Recall in predicting AIE

Methods	Top-1	Top-3	Top-5
Baseline (0)	0.231	0.266	*0.355*
Baseline (1)	0.165	0.225	0.300
Baseline (2)	0.180	0.288	0.306
NEURSA (0)	0.284	0.425	0.470
NEURSA (1)	0.291	0.358	0.403
NEURSA (2)	0.333	0.378	**0.489**
Gain	**0.489** - *0.355* = 0.134		

Table 7. F1 score in predicting AIE.

Methods	Top-1	Top-3	Top-5
Baseline (0)	*0.256*	0.169	0.163
Baseline (1)	0.188	0.149	0.145
Baseline (2)	0.196	0.183	0.136
NEURSA (0)	0.276	0.232	0.182
NEURSA (1)	0.299	0.195	0.157
NEURSA (2)	**0.347**	0.195	0.179
Gain	**0.347** - *0.256* = 0.091		

Table 8. Precision in predicting CCE.

Methods	Top-1	Top-3	Top-5
Baseline (0)	0.345	0.165	0.169
Baseline (1)	0.328	0.180	0.135
Baseline (2)	*0.352*	0.198	0.173
NEURSA (0)	0.362	0.220	0.170
NEURSA (1)	**0.438**	0.244	0.199
NEURSA (2)	**0.438**	0.252	0.193
Gain	**0.438** - *0.387* = 0.051		

Table 9. Recall in predicting CCE.

Methods	Top-1	Top-3	Top-5
Baseline (0)	0.270	0.319	0.467
Baseline (1)	0.319	0.369	0.393
Baseline (2)	0.291	0.371	*0.503*
NEURSA (0)	0.286	0.443	0.495
NEURSA (1)	0.292	0.413	0.486
NEURSA (2)	0.384	0.561	**0.620**
Gain	**0.620** - *0.503* = 0.117		

Table 10. F1 score in predicting CCE.

Methods	Top-1	Top-3	Top-5
Baseline (0)	0.303	0.217	0.249
Baseline (1)	*0.323*	0.242	0.201
Baseline (2)	0.319	0.258	0.257
NEURSA (0)	0.320	0.294	0.254
NEURSA (1)	0.350	0.307	0.282
NEURSA (2)	**0.409**	0.348	0.295
Gain	**0.409** - *0.323* = 0.086		

studied datasets in bug detection literature. Later we discover Infer does not have access to the build tools that are required to compile some of the projects in defect4j. Therefore, we show Infer's performance only on the projects it can compile. Those projects contain 58 bugs in total, namely Bug Set I.

First, we manually verify the validity, and more importantly, the location for all 75 bugs in case any bug may trigger an exception at a different location than developers' fix. Next, we feed the entire codebase of each project for each checker to scan. A report that points to a buggy location will be counted as a true positive, otherwise, it's a false positive. We acknowledge that a static analysis tool could have caught a real bug that is mistakenly counted as a false positive since it falls out of the 75 bugs we collected, however, the exact same issue applies to NEURSA, which we regrettably ignore due to resource constraint. We use NEURSA with depth 2 of inlining trained in the previous experiment. It is configured to run the top-1 prediction mode. We choose the most precise analysis for Pinpoint to perform. We also manually fine-tune BugPicker (*e.g.* increase the length of the call chain or reset the timeout), but obtain the same results. We do not manage to run any other configuration for Infer and SpotBugs rather than their default set up.

Table 11 depicts the results. Overall, we find (1) NEURSA achieves better precision and recall than any other evaluated tool; more importantly, (2) bugs that are found by competing tools are all caught by NEURSA. Besides, NEURSA detects another 11 bugs that are missed by the other tools.

Table 11. Results of the comparison. TP, FP, FN stand for true positives, false positives and false negatives respectively.

Tools	Bug Set I			Remaining Set			Total	
	TP	FP	FN	TP	FP	FN	Precision	Recall
FB Infer	4	1004	54	NA	NA	NA	.004	.069
Pinpoint	4	1524	54	3	1104	14	.003	.093
SpotBugs	0	107	58	1	26	16	.007	.013
BugPicker	0	79	58	0	0	17	0	0
NEURSA	16	1655	42	5	521	12	.010	.280

We have also applied NEURSA to catch bugs in the wild, and obtained encouraging results. Configured with top-1 prediction mode and inline depth of 2 (we also tried 3 and 4 for smaller methods), NEURSA found 50 bugs (40 NPE and 10 AIE) in 17 projects that are among the most starred on GitHub. All bugs are manually verified and reported to developers, out of which 7 are fixed and another 3 are confirmed (fixes pending). Our findings show that not only does NEURSA significantly improve the prior works, but more importantly, NEURSA is a industry-strength static tool in checking real-world Java projects.

5.6 Discussion on Limitation of NEURSA

In order to gain a deeper understanding of NEURSA's limitation, we mainly look into the bugs NEURSA missed in the prior experiment. We find that when bug patterns are not local, that is, the dereference is quite distant from where a null pointer is assigned, NEURSA tends

to struggle, in particular, it even misclassifies the method to be clean most of the time. The reason is, as one can imagine, NEURSA's signal gets diluted when a scattered bug pattern is overwhelmed by irrelevant statements in a program. We plan to tackle this issue with both program analysis and machine learning techniques. For data pre-processing, program slicing [35] seems to be a promising idea. Given the location of a potential null pointer dereference (due to the null assignment or non-initialization), we can filter out statements that fall out of the slice to localize a bug pattern. On the other hand, a larger, more diverse dataset that contains a variety of bug patterns should also help, or for data augmentation, we can synthesize new programs by randomly adding dummy statements in between the assignment and dereference of null pointer for buggy methods, especially when the high-quality, large-scale public datasets are unavailable.

Another issue we discovered is NEURSA is less accurate when handling large programs (*i.e.* approximately 1,000 nodes in the graph) despite the contribution IBPM makes to the underlying GNN. We find several bugs NEURSA missed where the bug patterns are in fact local. We believe this is due to the fundamental limitation of GNN, which requires deeper insight and understanding of the models themselves, without which, IBPM's results will be hard to improve upon in a qualitative manner.

We also briefly examine the false positives NEURSA emitted. For a few dozen we inspected, we find that the same issue causing NEURSA to miss bugs are also major sources of NEURSA's imprecision. In addition, NEURSA can be over-sensitive about the presence of null pointers, albeit we can not confirm they are never dereferenced.

6 Related Work

Machine Learning for Defect Prediction   Utilizing machine learning techniques for software defect prediction is another rapidly growing research field. So far the literature has been focusing on detecting simpler bugs that are syntactic in nature. Wang et al. [34] leverages deep belief network to learn program representations for defect prediction. Their model predicts an entire file to be buggy or not. Pradel and Sen [24] present Deepbugs, a framework to detect name-based bugs in binary operation. Another line of works targets variable misuse bugs [1, 33], in which developers use wrong variables, and models are required to predict the ones that should have been used. Clearly, NEURSA significantly differs from all of them as it locates complex semantic bugs.

Static Bug Finding   In principle, static analysis models all executions of a program in order to provide the soundness guarantee. However, perfectly sound static analysis tools almost never exist; concessions that sacrifice the soundness guarantee have to be made to ensure the usability of static analyzers. Several years ago, a new term—soundiness [21]—is brought forward aiming to clarify the level of approximation adopted in the analysis. Below we survey several flagship static analyzers.

SLAM [4], BLAST [14], and SATABS [8] adopt abstract refinement for static bug checking. CBMC [8, 9] performs bounded model checking. Saturn [10, 36] is another program analysis system, which uses the combination of summaries and constraints to achieve both high scalability and precision. Compass [11] performs bottom-up, summary-based heap analysis for the verification of real C and C++ programs.

Compared with static analysis tools, we believe NEURSA yields several conceptual advantages. First, with NEURSA, creating a static bug finder can be simplified to solving a machine learning task. In comparison, the traditional way of designing static analyzers even the unsound ones requires a substantial amount of human expertise. Besides, unlike the static analysis tools, model-based bug detectors can benefit from increasingly large datasets and powerful training regime, as a result, they will evolve and get better over time.

7 Conclusion

In this paper, we present NEURSA, a framework for creating neural bug detectors based on GNN. We also propose an interval-based propagation model to improve the capacity of GNN in learning program properties. Our evaluation shows that NEURSA is effective in catching semantic bugs; it outperforms several flagship static analyzers in catching null pointer dereference bugs; and even finds new bugs in many highly-rated and actively maintained projects on GitHub. For future work, we will apply the IBPM-Based GNN to other program analysis tasks as we believe our approach offers a general, and powerful framework for learning effective program analyzers.

References

[1] Miltiadis Allamanis, Marc Brockschmidt, and Mahmoud Khademi. 2017. Learning to represent programs with graphs. *arXiv preprint arXiv:1711.00740* (2017).

[2] Frances E. Allen. 1970. Control Flow Analysis. In *Proceedings of a Symposium on Compiler Optimization*. ACM, New York, NY, USA, 1–19. https://doi.org/10.1145/800028.808479

[3] Hagit Attiya and Jennifer Welch. 2004. *Distributed computing: fundamentals, simulations, and advanced topics*. Vol. 19. John Wiley & Sons.

[4] Thomas Ball and Sriram K. Rajamani. 2002. The SLAM Project: Debugging System Software via Static Analysis. *SIGPLAN Not.* 37, 1 (Jan. 2002), 1–3. https://doi.org/10.1145/565816.503274

[5] Josh Berdine, Cristiano Calcagno, and Peter W. O'Hearn. 2006. Smallfoot: Modular Automatic Assertion Checking with Separation Logic. In *Proceedings of the 4th International Conference on Formal Methods for Components and Objects (FMCO'05)*. Springer-Verlag, Berlin, Heidelberg, 115–137. https://doi.org/10.1007/11804192_6

[6] Cristiano Calcagno, Dino Distefano, Jeremy Dubreil, Dominik Gabi, Pieter Hooimeijer, Martino Luca, Peter O'Hearn, Irene Papakonstantinou, Jim Purbrick, and Dulma Rodriguez. 2015. Moving Fast with Software Verification. In *NASA Formal Methods*, Klaus Havelund, Gerard Holzmann, and Rajeev Joshi (Eds.). Springer International Publishing, Cham, 3–11.

[7] Kyunghyun Cho, Bart Van Merriënboer, Dzmitry Bahdanau, and Yoshua Bengio. 2014. On the properties of neural machine translation: Encoder-decoder approaches. *arXiv preprint arXiv:1409.1259* (2014).

[8] Edmund Clarke, Daniel Kroening, Natasha Sharygina, and Karen Yorav. 2004. Predicate Abstraction of ANSI-C Programs Using SAT. *Formal Methods in System Design* 25, 2 (01 Sep 2004), 105–127.

[9] Edmund Clarke, Daniel Kroening, and Karen Yorav. 2003. Behavioral Consistency of C and Verilog Programs Using Bounded Model Checking. In *Proceedings of the 40th Annual Design Automation Conference (DAC '03)*. ACM, New York, NY, USA, 368–371. https://doi.org/10.1145/775832.775928

[10] Isil Dillig, Thomas Dillig, and Alex Aiken. 2008. Sound, Complete and Scalable Path-sensitive Analysis. In *Proceedings of the 29th ACM SIGPLAN Conference on Programming Language Design and Implementation (PLDI '08)*. ACM, New York, NY, USA, 270–280. https://doi.org/10.1145/1375581.1375615

[11] Isil Dillig, Thomas Dillig, Alex Aiken, and Mooly Sagiv. 2011. Precise and Compact Modular Procedure Summaries for Heap Manipulating Programs. In *Proceedings of the 32Nd ACM SIGPLAN Conference on Programming Language Design and Implementation (PLDI '11)*. ACM, New York, NY, USA, 567–577. https://doi.org/10.1145/1993498.1993565

[12] Marco Gori, Gabriele Monfardini, and Franco Scarselli. 2005. A new model for learning in graph domains. In *Proceedings. 2005 IEEE International Joint Conference on Neural Networks, 2005.*, Vol. 2. IEEE, 729–734.

[13] Andrew Habib and Michael Pradel. 2018. How Many of All Bugs Do We Find? A Study of Static Bug Detectors. In *Proceedings of the 33rd ACM/IEEE International Conference on Automated Software Engineering (ASE 2018)*. ACM, New York, NY, USA, 317–328. https://doi.org/10.1145/3238147.3238213

[14] Thomas A. Henzinger, Ranjit Jhala, Rupak Majumdar, and Grégoire Sutre. 2002. Lazy Abstraction. In *Proceedings of the 29th ACM SIGPLAN-SIGACT Symposium on Principles of Programming Languages (POPL '02)*. ACM, New York, NY, USA, 58–70. https://doi.org/10.1145/503272.503279

[15] David Hovemeyer and William Pugh. 2004. Finding Bugs is Easy. *SIGPLAN Not.* 39, 12 (Dec. 2004), 92–106.

[16] L. Jiang, G. Misherghi, Z. Su, and S. Glondu. 2007. DECKARD: Scalable and Accurate Tree-Based Detection of Code Clones. In *29th International Conference on Software Engineering (ICSE'07)*. 96–105. https://doi.org/10.1109/ICSE.2007.30

[17] René Just, Darioush Jalali, and Michael D Ernst. 2014. Defects4J: A database of existing faults to enable controlled testing studies for Java programs. In *Proceedings of the 2014 International Symposium on Software Testing and Analysis*. ACM, 437–440.

[18] Diederik P Kingma and Jimmy Ba. 2014. Adam: A method for stochastic optimization. *arXiv preprint arXiv:1412.6980* (2014).

[19] Yujia Li, Daniel Tarlow, Marc Brockschmidt, and Richard Zemel. 2015. Gated graph sequence neural networks. *arXiv preprint arXiv:1511.05493* (2015).

[20] Yaguang Li, Rose Yu, Cyrus Shahabi, and Yan Liu. 2017. Diffusion convolutional recurrent neural network: Data-driven traffic forecasting. *arXiv preprint arXiv:1707.01926* (2017).

[21] Benjamin Livshits, Manu Sridharan, Yannis Smaragdakis, Ondřej Lhoták, J Nelson Amaral, Bor-Yuh Evan Chang, Samuel Z Guyer, Uday P Khedker, Anders Møller, and Dimitrios Vardoulakis. 2015. In defense of soundness: a manifesto. *Commun. ACM* 2 (2015), 44–46.

[22] Tomas Mikolov, Kai Chen, Greg Corrado, and Jeffrey Dean. 2013. Efficient estimation of word representations in vector space. *arXiv preprint arXiv:1301.3781* (2013).

[23] Renaud Pawlak, Martin Monperrus, Nicolas Petitprez, Carlos Noguera, and Lionel Seinturier. 2015. Spoon: A Library for Implementing Analyses and Transformations of Java Source Code. *Software: Practice and Experience* 46 (2015), 1155–1179. https://doi.org/10.1002/spe.2346

[24] Michael Pradel and Koushik Sen. 2018. Deepbugs: a learning approach to name-based bug detection. *Proceedings of the ACM on Programming Languages* 2, OOPSLA (2018), 147.

[25] Caitlin Sadowski, Jeffrey van Gogh, Ciera Jaspan, Emma Söderberg, and Collin Winter. 2015. Tricorder: Building a Program Analysis Ecosystem. In *Proceedings of the 37th International Conference on Software Engineering*.

[26] Ripon Saha, Yingjun Lyu, Wing Lam, Hiroaki Yoshida, and Mukul Prasad. 2018. Bugs. jar: a large-scale, diverse dataset of real-world java bugs. In *2018 IEEE/ACM 15th International Conference on Mining Software Repositories (MSR)*. IEEE, 10–13.

[27] Franco Scarselli, Marco Gori, Ah Chung Tsoi, Markus Hagenbuchner, and Gabriele Monfardini. 2008. The graph neural network model. *IEEE Transactions on Neural Networks* 20, 1 (2008), 61–80.

[28] Andrew Scott, Johannes Bader, and Satish Chandra. 2019. Getafix: Learning to fix bugs automatically. *Proc. ACM Program. Lang.* 2, OOPSLA.

[29] Qingkai Shi, Xiao Xiao, Rongxin Wu, Jinguo Zhou, Gang Fan, and Charles Zhang. 2018. Pinpoint: fast and precise sparse value flow analysis for million lines of code. In *Proceedings of the 39th ACM SIGPLAN Conference on Programming Language Design and Implementation*. ACM, 693–706.

[30] Xujie Si, Hanjun Dai, Mukund Raghothaman, Mayur Naik, and Le Song. 2018. Learning loop invariants for program verification. In *Advances in Neural Information Processing Systems*. 7751–7762.

[31] Daniel Svozil, Vladimir Kvasnicka, and Jiri Pospichal. 1997. Introduction to multi-layer feed-forward neural networks. *Chemometrics and intelligent laboratory systems* 39, 1 (1997), 43–62.

[32] David A Tomassi, Naji Dmeiri, Yichen Wang, Antara Bhowmick, Yen-Chuan Liu, Premkumar T Devanbu, Bogdan Vasilescu, and Cindy Rubio-González. 2019. Bugswarm: mining and continuously growing a dataset of reproducible failures and fixes. In *2019 IEEE/ACM 41st International Conference on Software Engineering (ICSE)*. IEEE, 339–349.

[33] Ashish Vaswani, Noam Shazeer, Niki Parmar, Jakob Uszkoreit, Llion Jones, Aidan N Gomez, Lukasz Kaiser, and Illia Polosukhin. 2017. Attention is all you need. In *Advances in neural information processing systems*. 5998–6008.

[34] Song Wang, Taiyue Liu, and Lin Tan. 2016. Automatically learning semantic features for defect prediction. In *2016 IEEE/ACM 38th International Conference on Software Engineering (ICSE)*. IEEE, 297–308.

[35] Mark Weiser. 1981. Program Slicing. In *Proceedings of the 5th International Conference on Software Engineering (ICSE '81)*. IEEE Press, Piscataway, NJ, USA, 439–449. http://dl.acm.org/citation.cfm?id=800078.802557

[36] Yichen Xie and Alex Aiken. 2005. Scalable Error Detection Using Boolean Satisfiability. In *Proceedings of the 32Nd ACM SIGPLAN-SIGACT Symposium on Principles of Programming Languages (POPL '05)*. ACM, New York, NY, USA, 351–363. https://doi.org/10.1145/1040305.1040334

[37] Danfei Xu, Yuke Zhu, Christopher B Choy, and Li Fei-Fei. 2017. Scene graph generation by iterative message passing. In *Proceedings of the IEEE Conference on Computer Vision and Pattern Recognition*. 5410–5419.

[38] Xin Ye, Razvan Bunescu, and Chang Liu. 2014. Learning to rank relevant files for bug reports using domain knowledge. In *Proceedings of the 22nd ACM SIGSOFT International Symposium on Foundations of Software Engineering*. ACM, 689–699.

[39] Rex Ying, Ruining He, Kaifeng Chen, Pong Eksombatchai, William L. Hamilton, and Jure Leskovec. 2018. Graph Convolutional Neural Networks for Web-Scale Recommender Systems. In *Proceedings of the 24th ACM SIGKDD International Conference on Knowledge Discovery & Data Mining (KDD '18)*. ACM, New York, NY, USA, 974–983.